systems

MDPI

Article

A Green Flexible Job-Shop Scheduling Model for Multiple AGVs Considering Carbon Footprint

Xinxin Zhou [1], Fuyu Wang [1,2,*], Nannan Shen [1] and Weichen Zheng [1]

[1] School of Management Science and Engineering, Anhui University of Technology, Ma'anshan 243032, China; student_xiaozhou@163.com (X.Z.)
[2] Key Laboratory of Multidisciplinary Management and Control of Complex Systems of Anhui Higher Education Institutes, Anhui University of Technology, Ma'anshan 243032, China
* Correspondence: ahutwfy@ahut.edu.cn

Abstract: Green and low carbon automated production has become a research hotspot. In this paper, the AGV transport resource constraint, machine layout and job setup time have been integrated into the background of a flexible job shop. From a whole life-cycle perspective, the AGV allocation strategy has been formulated by simulating multiple scenarios within the production system. Aimed at makespan, carbon footprint, and machine load, a green low-carbon flexible job shop scheduling model with multiple transport equipment (GFJSP-MT) has been constructed. To address this problem, a relevant case dataset was formed, and a heuristic strategy NSGA-II using a real number encoded embedded cycle to replace repeated individuals was proposed. Through longitudinal and horizontal comparisons, the effectiveness of the AGV allocation strategy has been verified and the optimum number of AGVs in the case determined. Finally the quality and diversity of the Pareto frontier solutions are compared and the scheduling scheme for each sub-objective are discussed. The results show that the model and algorithm constructed in this paper can effectively achieve the optimal scheduling of green flexible shop production.

Keywords: flexible job shop; limited AGV transport; carbon footprint; NSGA-II

Citation: Zhou, X.; Wang, F.; Shen, N.; Zheng, W. A Green Flexible Job-Shop Scheduling Model for Multiple AGVs Considering Carbon Footprint. *Systems* **2023**, *11*, 427. https://doi.org/10.3390/systems11080427

Academic Editor: Vladimír Bureš

Received: 2 July 2023
Revised: 28 July 2023
Accepted: 9 August 2023
Published: 14 August 2023

1. Introduction

In light of global economic, population, and societal changes, the occurrence of environmental pollution, climate warming, and energy scarcity has become increasingly frequent. Consequently, there is a growing focus on green and low-carbon initiatives. Given the manufacturing industry's high energy consumption and emissions, it is imperative to explore a low-carbon transformation path that transcends the previously prioritized economic and technical cost indicators, such as makespan and total machine load.

Moreover, the development of artificial intelligence (AI) has ushered in a range of new technologies, including reinforcement learning, which has significantly propelled the advancement of intelligent manufacturing in the context of Industry 4.0 [1]. Coupled with the challenges posed by the green and low-carbon movement, the manufacturing industry is progressively transitioning towards a sustainable Industry 5.0, emphasizing the consideration of human factors and the environment, as well as a shift towards diverse product offerings and small-batch personalized production [2].

One approach that aligns with this paradigm shift is the adoption of Flexible Job Shop (FJS) scheduling, which accounts for multiple jobs, machines, and uncertainties regarding job processing machines. FJS enhances production flexibility and partially adheres to the personalized production mode characterized by multiple varieties and small batches. Destouet et al. [2] conducted a review survey of flexible job shop scheduling problems (FJSP) involving human and environmental factors. In this article, the authors selected 135 papers from 2013 onwards, of which 101 considered environmental factors, 100 of 101 concerned energy consumption and 22 concerned carbon emissions. This observation

underscores the increasing prominence of research pertaining to production modes that account for green indicators such as energy consumption and carbon emissions within the manufacturing industry.

Duan and Wang [3] proposed a heuristic non-dominated sorting genetic algorithm (NSGA-II) embedded with batch transportation rules for dynamic FJSP with machine breakdowns, comprehensive consideration of machine on/off, and machine multi-speed selection, aiming at makespan and energy consumption. Galdeira et al. [4] considered the FJSP of new job arrivals and machine on/off comprehensively and designed an improved backtracking search algorithm embedded in an insertion rescheduling strategy with the objectives of makespan, energy consumption, and instability. Gong et al. [5] realized energy efficient by controlling machine on/off, and designed a two-stage memetic algorithm aiming to makespan, energy consumption and number of machine restarts. Lei et al. [6] researched makespan and total tardiness under energy consumption threshold constraints and proposed a two-stage meta-heuristic algorithm integrating an imperialist competitive algorithm and variable neighborhood search. Wei et al. [7] considered the problem of energy consumption for machines with variable machining speeds, developed energy-aware model for different states of the machine, and designed multiple energy-saving scheduling measures. Wu et al. [8] similarly designed NSGA-II targeting makespan and energy consumption for the FJSP with variable machining speeds. Zhang et al. [9] developed a multi-objective hybrid algorithm for solving the FJSP considering makespan, setup time and energy consumption. Jiang and Deng [10] proposed an improved bi-population discrete cat swarm algorithm using the sum of machine energy consumption cost and earliness/tardiness cost as the objective. Ning et al. [11] proposed a quantum bacterial foraging optimization algorithm targeting makespan, total machine load and total energy consumption. Yin et al. [12] proposed a genetic algorithm based on a simplex lattice for solving the FJSP with makespan, total energy consumption, and noise emissions as the objectives. Many scholars consider not only energy consumption indicators, but also carbon emissions as a green indicator by analyzing the level of carbon emission factors.

Zhu et al. [13] proposed a memetic algorithm with the four neighborhood structures based on the Low Carbon FJSP for Worker Learning (LFJSP-WL) with makespan, total carbon emissions and total worker cost as the objectives. Seng et al. [14] effectively demonstrated that decoding based on low carbon emissions can be compatible with the strengths of decoding based on the makespan and energy consumption. Piroozfard et al. [15] designed a multi-objective genetic algorithm for FJSP with carbon footprint and total tardiness as the objectives, and demonstrated the effectiveness of the algorithm through multi-dimensional indicators. Workshop production as an entirety, some scholars take a holistic view of the whole life cycle, considering all carbon emissions produced by the jobs from entering the workshop until machining is completed, i.e., the carbon footprint. Jiang et al. [16] developed a low-carbon flexible job shop scheduling model by comprehensively considering the carbon emissions produced from machine energy consumption, tool wear and cutting fluid. Liu et al. [17] designed an improved NSGA-II aimed at makespan and carbon footprint by considering the carbon emissions caused by machines, jobs transportation, machining swarf, and machining materials. Wen et al. [18] proposed an improved NSGA-II based on the N5 neighborhood search, considering the carbon emissions produced from the machine, job setup time, coolant, and lubricant consumption.

The above-mentioned studies considered energy consumption and carbon emissions in various scenarios from the machine level, but rarely the transport of jobs, which has been increasingly considered between machines in order to better reproduce the actual production situation.

Li and Lei [19] proposed a feedback imperialist competitive algorithm with the objectives of makespan, tardiness, and energy consumption by integrating the FJSP, which considers transportation, sequence-dependent setup time. Jiang et al. [20] investigated the FJSP with a simultaneous job transportation and deterioration effect, aiming at total energy consumption. Li et al. [21] comprehensively considered the transportation resources

and job setup time constraints, and proposed an improved artificial bee colony algorithm with makespan and total energy consumption as the objectives. Dai et al. [22] constructed a multi-situational energy-aware model for FJSP with AGV transportation resource constraints and demonstrated that the transportation time was positively correlated to the overall objective. Wang et al. [23] developed an improved NSGA-II for FJSP with job transportation constraints, aiming at makespan, total tardiness and energy consumption.

While the studies mentioned above considered the transport of jobs between machines, the models have frequently been simplified by making assumptions such as infinite amounts of transport equipment and that the front or back operation of the jobs are not involved in the transport, which may to a certain extent be a deviation from actual production. Li et al. [24] creatively embed machine layout rearrangement, transport equipment allocation and worker assignment in the study of job shop scheduling problem (JSP). Zhang et al. [25] similarly embedded limited AGV transport in the study of energy-efficient FJSP with contingencies.

In summary, it can be seen that studies on FJSP need to consider not only traditional economic and technical cost indicators such as makespan, but also environmental indicators such as energy consumption. However, there are not many studies that consider the carbon emissions and carbon footprint, and the research focus is mostly on the machine level, while studies focusing on the finite amounts of transport equipment allocation and jobs machining processes are still insufficient.

Hence, based on previous studies, the major contributions of this paper are as follows:

(1) In this paper, a Green Low-Carbon Flexible Job Shop Scheduling Model with Multiple Transport Equipment (GFJSP-MT) is constructed integrating machine layout, limited transport equipment allocation, job transport time, job setup time and various types of machining material consumption with the objectives of makespan, total machine load and total carbon footprint.
(2) AGV allocation strategy is developed based on various mixed scenarios in the job machining process.
(3) A heuristic strategy NSGA-II is designed to address the inadequacy of the traditional NSGA-II elite solution selection strategy, which has been embedded to obtain new individuals to replace duplicate individuals with the crowding distance of zero using cross-mutation between elite pool solutions.
(4) In response to the need for model, this paper has been developed on the basis of previous research, and the case data set is expanded to form a model benchmark case set for further research by scholars.

In this paper, the research contents are arranged as follows: Section 2 constructs a mathematical model of the integrated multi-factor GFJSP-MT and develops an AGV allocation strategy. Section 3 is focused on improved operational operators for NSGA-II. Section 4 is a detailed experimental case study. Conclusions and outlooks are given in Section 5.

2. Model Construction

2.1. Problem Description

Before formulating the problem, some symbols are defined as follows in Table 1.

Table 1. Definition of symbols.

n	The total number of jobs.
m	The total number of machines.
v	The total number of AGVs.
i,i', h	The index of jobs i,i', h =1, 2, . . . , n.
j,j', l	The index of operations j,j', l =1, 2, . . . , R_i.
k, w	The index of machines k, w =0, 1, 2, . . . , m, m+1. (When k, w =0 or m+1 denotes the material center and product staging area respectively.)
u	The index of AGVs u =0, 1, 2, . . . , v. (When u =0, there is no necessary to allocate AGV to operation O_{ij}.)
O_{ij}	The operation j of job J_i.
R_i	The set of operations for J_i.
W	The set of machining power of the machine.
Q	The set of idle power of the machine.
p_u	The u-th AGV load power.
q	The AGVs no-load power.
F	The set of unused machines, $F \in M$.
ED_{kw}	Euclidean distance between machines
QS_{ij}	Swarf quality after machining.
QL_{ijk}	Lubricants consumed per unit time of O_{ij} on machine k.
QC_{ijk}	Coolants consumed per unit time of O_{ij} on machine k.
TT_{uij}	AGV current transport task completion time
$TT_{uijk'w}$	The no-load transport time between the current machine k' and machine w, in order to transport the operation O_{ij} by the AGV.
TT_{uijwk}	The load transport time of the AGV's transport operation O_{ij} between machine w and machine k.
TC_{ijk}	Clamping time of operation O_{ij}.
TD_{ijk}	Disassembly time of operation O_{ij}.
S_{ij}	Starting time of operation O_{ij}.
C_{ij}	Completion time of operation O_{ij}.
t_{ijk}	Processing time of operation O_{ij}.
C_i	Completion time of job J_i.
C_{max}	Makespan.
CF	Total carbon footprint.
ML	Total machine load.
EF_α	Carbon emission factor
x_{ijk}	$x_{ijk} = 1$, operation O_{ij} processed on machine k, otherwise $x_{ijk} = 0$.
x_{iju}	$x_{iju} = 1$, operation O_{ij} transported by the u-th AGV, otherwise $x_{iju} = 0$.
y_{ijhlk}	$y_{ijhlk} = 1$, operation O_{hl} is processed on machine k before O_{ij}, otherwise $y_{ijhlk} = 0$.
z_{ijhlk}	$z_{ijhlk} = 0$, adjacent machining tasks on machine k are adjacent operations of the same job, otherwise $z_{ijhlk} = 1$, where O_{ij} is processed after O_{hl}.
L	A great positive number

There are a set of jobs $J = \{J_1, J_2, \ldots, J_n\}$ and a set of machines $M = \{M_1, M_2, \ldots, M_m\}$ and a set of AGVs $V = \{V_1, V_2, \ldots, V_v\}$. Each J_i contains of operations $R_i = \{O_{i1}, O_{i2}, \ldots, O_{ij}\}$. Each operation O_{ij} can be processed on any one machine of a set of available machines $M_{ij} \in M$ and transported by an AGV $v \in V$ to the machine $k \in M_{ij}$. During the processing of the job, it is necessary to take into account the clamping and disassembly time before and after the processing of the operation O_{ij}. Simultaneously, job swarf is produced and lubricants and coolants are consumed.

For this GFJSP-MT model, some assumptions are made as follows:

(1) Both the jobs and the AGVs are simultaneously available at zero time and located in the material center.
(2) All machines are powered on at zero time until all process jobs on that machine are completed and then the machine is powered off.
(3) Allow the machine to have no jobs, then the machine will be in idle mode until all jobs have been processed.

(4) Each AGV can only transport one job at a time.
(5) Each job can only be processed by one machine, and the machine can only process one job, and processing cannot be interrupted.
(6) Jobs and machines are independent, i.e., there is no interdependency between different jobs or machines. However, precedence relationships or technological sequences between operations of the same job must be considered.
(7) When the job J_i is transported by the AGV to machine k, if the previous job of the machine has not yet been completed, the job is stored in the pending processing area of the machine, and the AGV is released at that time.
(8) When all jobs are completed, the jobs are transported by AGV to product staging area, then all AGVs return to the material center.

2.2. AGV Allocation Strategy

In this model, AGVs perform a significant role, undertaking on the transport of the entire scheduling task. In order to correctly allocate AGVs to the operation O_{ij}, this paper formulates an AGV allocation strategy based on the following principles.

(1) When the job J_i is not machined for the first time, it is necessary to consider whether the machine k is machining operation $O_{i(j-1)}$ and O_{ij} continuously, i.e., when $z_{ijhlk} = 0$, there is no need to allocate AGVs, while correcting for $C_{i(j-1)}$ and $TD_{i(j-1)k}$.
(2) When $z_{ijhlk} = 1$, it means that adjacent machining tasks of machine k are not the same job J_i, then it is necessary to determine whether $O_{i(j-1)}$ and O_{ij} are processed on the same machine, i.e., whether $x_{ijk} = x_{i(j-1)k}$ are equal. If the condition is true, no AGVs should be allocated to operation O_{ij}.

Besides the above, other operations O_{ij} need to transport the job by AGV before and after processing, as shown in Figure 1.

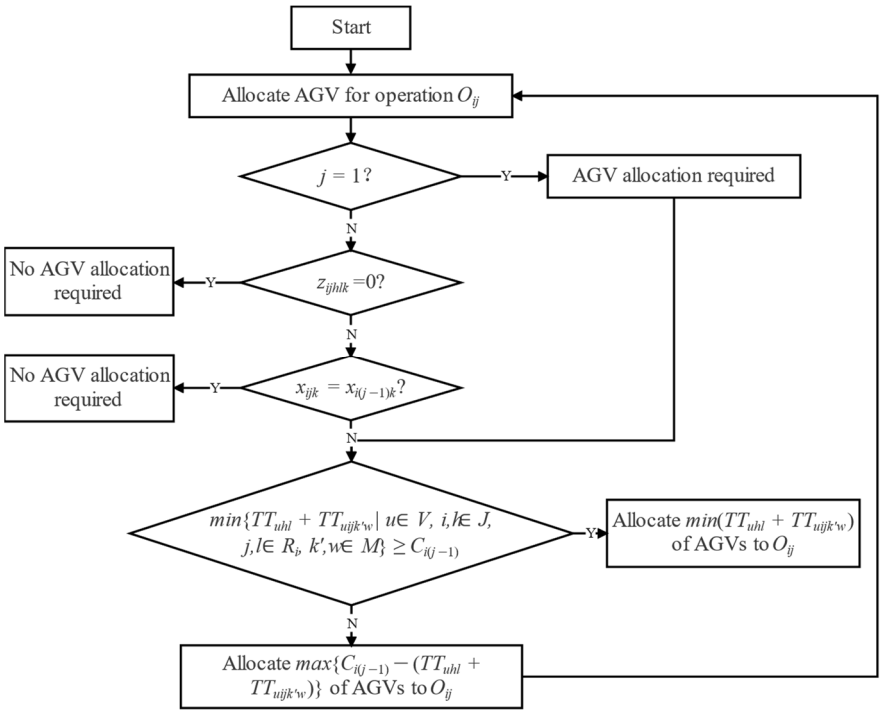

Figure 1. AGV allocation strategy in multiple scenarios.

For each AGV, the magnitude of the relationship between the sum of the end time of the previous transport task (TT_{uhl}) and the idle time from the current machine k' to machine w ($TT_{uijk'w}$) and the completion time ($C_{i(j-1)}$) of operation $O_{i(j-1)}$ is determined.

When the sum of TT_{uhl} and $TT_{uijk'w}$ of all AGVs is greater than $C_{i(j-1)}$, i.e., $min\left\{TT_{uhl} + TT_{uijk'w} | u \in V;\ i,\ j \in J;\ h,\ l \in R_i;\ k',\ w \in M\right\} \geq C_{i(j-1)}$, at which point, for each AGV, operation $O_{i(j-1)}$ has been already completed processing or just completed processing when the AGV arrives at machine w without load, and the job is in the machine staging area waiting to be transported. When the above conditions are true, select the AGV with the $min\left(TT_{uhl} + TT_{uijk'w}\right)$. Otherwise, to improve the utilization of the AGVs without increasing the waiting transportation time of the job, select the AGV with the $max\left\{C_{i(j-1)} - \left(TT_{uhl} + TT_{uijk'w}\right)\right\}$.

2.3. GFJSP-MT Model

Naturally, in this GFJSP-MT model, the carbon footprint is divided into five parts, i.e., carbon emissions from machine process (PCE) and idle (ICE), transport (TCE), swarf (SCE), lubricants (LCE) and coolants (CCE).

2.3.1. Carbon Footprint

1. Carbon emissions from processing/idling

Carbon emissions from machines in this paper are derived from the electrical energy consumed by machines during processing and idling. Where PCE is the carbon emission created by the processing of O_{ij}, as shown in Equation (1).

$$PCE = \sum_{k=1}^{m} \sum_{i=1}^{n} \sum_{j=1}^{R_i} x_{ijk} t_{ijk} W_k EF_{\alpha_1} \tag{1}$$

As for ICE it is necessary to consider the machine idle waiting times, such as the transport, clamping and disassembly times of O_{ij} and the presence of unused machines, so the calculation is presented in Equation (2).

$$ICE = \left[\begin{array}{l} \sum\limits_{k=1}^{m} \sum\limits_{i=1}^{n} \sum\limits_{j=1}^{R_i} x_{ijk} Q_k \left(S_{ij} - y_{ijhlk} C_{hl} + z_{ijhlk} TD_{hlk}\right) + \\ \sum\limits_{f \in F} Q_f \left(C_{max} - TT_{u(i=max)(R_i+1)(k'w)} - TT_{u(i=max)(R_i+1)(w \to m+1)}\right) \end{array} \right] EF_{\alpha_1} \tag{2}$$

2. Carbon emissions from transport

There are three main parts to the carbon emissions caused by AGVs transport, as shown in Equation (3).

$$TCE = \left[\sum_{u=1}^{v} \sum_{i=1}^{n} \sum_{j=1}^{(R_i+1)} x_{iju} p_u TT_{uijwk} + \sum_{u=1}^{v} \sum_{i=1}^{n} \sum_{j=1}^{R_i} x_{iju} q TT_{uijk'w} + \sum_{u=1}^{v} q TT_{u(m+1 \to 0)} \right] EF_{\alpha_1} \tag{3}$$

The first part is the carbon emission from the AGV's load transport O_{ij}. As Assumption (8) stipulates that the job has to be transferred to the product staging area after completed, so the job requires an additional transport task to the product staging area, i.e., $R_i + 1$. The second part is the carbon emission from the AGV's no-load transport at the current machine k' and machine w. The third part is the carbon emission from the AGVs return to the material center.

3. Carbon emissions from swarf

After O_{ij} has been machined, there will be a loss of quality, i.e., swarf, and this part of the swarf will also cause carbon emissions. Assuming that the swarf in machining

does not vary with the machine, then this carbon emission will be a constant, as shown in Equation (4).

$$SCE = \sum_{i=1}^{n} \sum_{j=1}^{R_i} QS_{ij} EF_{\alpha_2} \tag{4}$$

4. Carbon emissions from lubricants and coolants

Lubricants and coolants are consumed during O_{ij} machining. Assuming O_{ij} machining, the amount of lubricant and coolant consumed per unit time varies with the machine. Therefore, the carbon emissions from lubricant and coolant consumption are shown in Equations (5) and (6), respectively.

$$LCE = \sum_{k=1}^{m} \sum_{i=1}^{n} \sum_{j=1}^{R_i} x_{ijk} t_{ijk} QL_{ijk} EF_{\alpha_3} \tag{5}$$

$$CCE = \sum_{k=1}^{m} \sum_{i=1}^{n} \sum_{j=1}^{R_i} x_{ijk} t_{ijk} QC_{ijk} EF_{\alpha_4} \tag{6}$$

Summing up, the $CF = PCE + ICE + TCE + LCE + CCE$.

2.3.2. Makespan

Previously it has been described how to account for the carbon footprint in the GFJSP-MT model. However, calculation of various types of carbon emissions is subject to time constraints such as S_{ij} and C_{ij}.

As both the setup time and transport time of the job and the end of the AGV current transport task are considered in the GFJSP-MT model, so multiple comparisons are required to determine the S_{ij}, as shown in Equation (7).

$$S_{ij} = \begin{cases} TT_{uhl} + TT_{uijk'w} + TT_{uijwk} + TC_{ijk} \\ \text{when}\Big(\Big(TT_{uhl} + TT_{uijk'w} \geq C_{i(j-1)}\Big) \& \Big(TT_{uhl} + TT_{uijk'w} + TT_{uijwk} \geq C_{i'j'}\Big)\Big) \\ C_{i(j-1)} + TT_{uijwk} + TC_{ijk} \\ \text{when}\Big(\Big(TT_{uhl} + TT_{uijk'w} < C_{i(j-1)}\Big) \& \Big(C_{i(j-1)} + TT_{uijwk} \geq C_{i'j'}\Big)\Big) \\ C_{i'j'} + TC_{ijk} \\ \text{when}\Big(\Big(TT_{uhl} + TT_{uijk'w} + TT_{uijwk} < C_{i'j'}\Big) \Big| \Big(C_{i(j-1)} + TT_{uijwk} < C_{i'j'}\Big)\Big) \\ C_{hl} \\ \text{when}\Big(z_{ijhlk} = 0\Big) \\ C_{hl} + TC_{ijk} \\ \text{when}\Big(\Big(z_{ijhlk} = 1\Big) \& \Big(x_{ijk} = x_{i(j-1)k}\Big)\Big) \end{cases} \tag{7}$$

Equation (7) discussed S_{ij} in two parts, where the first part was O_{ij} required AGV transportation, and the second part was O_{ij} not required AGV transportation. As an example, taking the first case of the first part, when the u-th AGV has finished the previous transport task and without load to machine w, the processing of $O_{i(j-1)}$ has not yet been completed, i.e., $TT_{uhl} + TT_{uijk'w} \geq C_{i(j-1)}$, whereas when the O_{ij} has been transported by the AGV from machine w to machine k, the previous machining task on machine k has not yet been completed, i.e., $TT_{uhl} + TT_{uijk'w} + TT_{uijwk} \geq C_{i'j'}$. At this point, $S_{ij} = TT_{uhl} + TT_{uijk'w} + TT_{uijwk} + TC_{ijk}$. Similarly, the other cases are not elaborated in this paper.

Based on the discussion of the multiple cases of S_{ij} and the model assumptions, C_{hl}, C_{ij} and TT_{uij} can be further obtained as shown in Equations (8) and (9), respectively.

$$\begin{aligned} C_{hl} &= S_{hl} + x_{hlk} t_{hlk} + z_{ijhlk} TD_{hlk} \\ C_{ij} &= S_{ij} + x_{ijk} t_{ijk} + TD_{ijk} \end{aligned} \tag{8}$$

Note that C_{hl} and TD_{hlk} in Equation (8) have to be corrected forward according to Figure 1, i.e., when $z_{ijhlk} = 0$, there is no need to allocate AGV for O_{ij}, at which point $C_{hl} = S_{hl} + x_{hlk}t_{hlk}$ and $TD_{hlk} = 0$.

$$TT_{uij} = \begin{cases} TT_{uhl} + TT_{uijk'w} + TT_{uijwk} \\ \text{when}\left(TT_{uhl} + TT_{uijk'w} \geq C_{i(j-1)}\right) \\ C_{i(j-1)} + TT_{uijwk} \\ \text{when}\left(TT_{uhl} + TT_{uijk'w} < C_{i(j-1)}\right) \end{cases} \tag{9}$$

In summary, C_i and C_{max} are given in Equation (10).

$$\begin{aligned} C_i &= \sum_{j=1}^{R_i} C_{ij} + TT_{ui(R_i+1)(k'w)} + TT_{ui(R_i+1)(w\to m+1)} \\ C_{max} &= \max_{i\in J} C_i \end{aligned} \tag{10}$$

2.3.3. Total Machine Load

The total machine load (ML) refers to the total time the job has been on the machine and reflects the overall machine utilization, as shown in Equation (11).

$$ML = \sum_{k=1}^{m}\sum_{i=1}^{n}\sum_{j=1}^{R_i} x_{ijk}t_{ijk} \tag{11}$$

2.3.4. Comprehensive Optimization Model

A multi-objective optimization model for GFJSP-MT is shown in Equation (12), where carbon footprint is used a green indicator and completion time and total machine load are used as economic indicators.

$$f = \min(C_{max}, CF, ML) \tag{12}$$

$$Subject\ to: \begin{cases} S_{ij} + x_{ijk}t_{ijk} + TD_{ijk} \leq C_{ij} \\ C_{ij} \leq S_{i(j+1)} \end{cases} \tag{13}$$

$$\sum_{k=1}^{m} x_{ijk} = 1 \tag{14}$$

$$\sum_{u=1}^{v} x_{iju} = 1 \tag{15}$$

$$C_{hl} \leq S_{ij} + L\left(1 - y_{ijhlk}\right) \tag{16}$$

$$TT_{uhl} + TT_{uijk'w} + TT_{uijwk} \leq TT_{uij} \tag{17}$$

$$x_{ijk} = \begin{cases} 1, \text{operation } O_{ij} \text{ processed on machine } k \\ 0, \text{otherwise} \end{cases} \tag{18}$$

$$x_{iju} = \begin{cases} 1, \text{operation } O_{hl} \text{ transported by the } u\text{-th AGV} \\ 0, \text{otherwise} \end{cases} \tag{19}$$

$$y_{ijhlk} = \begin{cases} 1, \text{operation } O_{hl} \text{ is processed on machine } k \text{ before } O_{ij} \\ 0, \text{otherwise} \end{cases} \tag{20}$$

$$z_{ijhlk} = \begin{cases} 0, \text{adjacent operations on machine } k \text{ are the same job} \\ 1, \text{otherwise} \end{cases} \quad (21)$$

Equation (13) indicates that job processing is subject to process priority, Equation (14) is the decision variable indicating that the same job can only be processed by one machine at the same time, Equation (15) show that the same job can only be transported by one AGV at the same time, Equation (16) means that only one job can be processed by the same machine at the same time, Equation (17) indicates that only one job can be transported by one AGV at the same time, Equations (18)–(21) are the constraints of the decision variable.

3. An Improved NSGA-II for Solving GFJSP-MT

Non-Dominated Sorting Genetic Algorithm (NSGA-II) was proposed by Deb et al. [26] as an improvement on NSGA, which has been widely used in the field of multi-objective job shop scheduling due to its ingenious mechanism of non-dominated sorting and crowding distance, which allows for an excellent robustness and solving ability. Nevertheless, there are still inadequacies in NSGA-II, such as the diversity and quality deficits of Pareto front solutions due to its elite solution selection strategy.

On this basis, an improved NSGA-II solving GFJSP-MT is proposed in this paper, and the algorithm framework is shown in Figure 2 following which the key components are described.

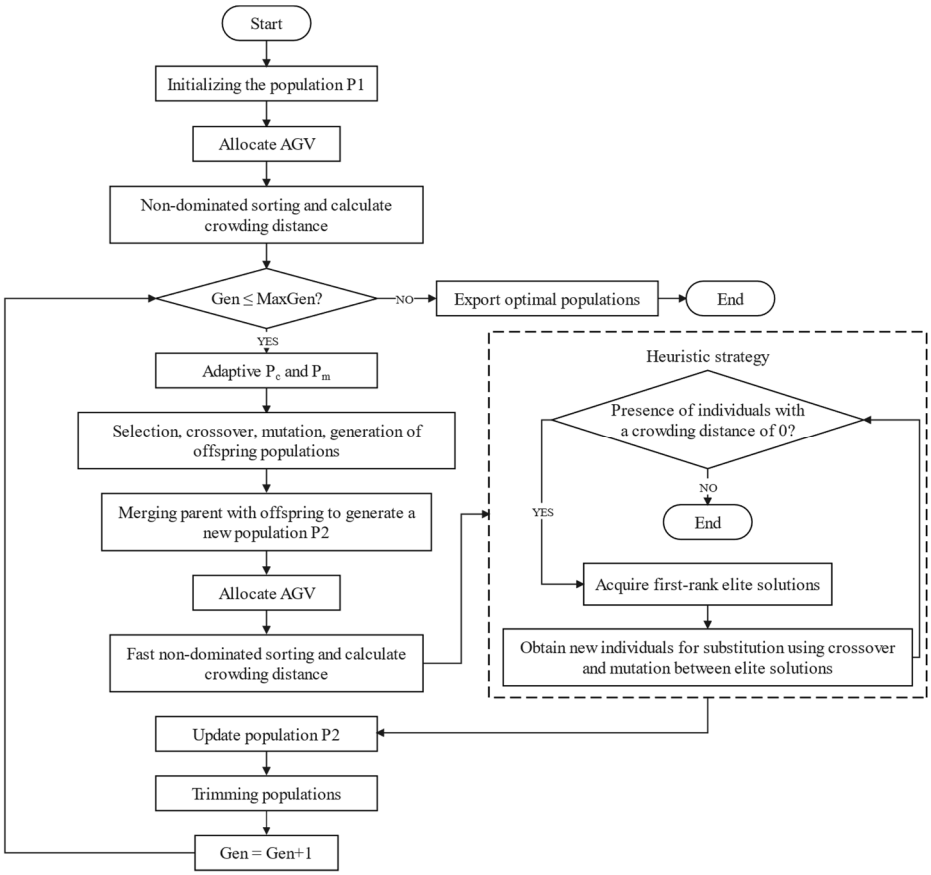

Figure 2. Improved flow of the NSGA-II algorithm.

3.1. Encoding and Decoding

In this paper, the GFJSP-MT is encoded in a real number format, which specifically includes two parts: operation sort (OS) and machine selection (MS), as shown in Figure 3.

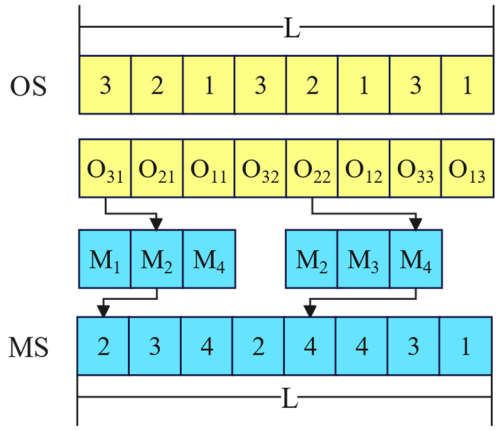

Figure 3. Method of individual encoding.

Where the real number in OS represents job_i, such as 3 for job_3, and the number of occurrences represents the number of operations corresponding to the job, for example, the first 3 indicates the first operation of job_3, i.e., O_{31}, and the second 2 indicates the second operation of job_2, i.e., O_{22}. Real number in MS represents the machine corresponding to the operation, for example, the set of available machines M_{ij} for O_{31} is $\{M_1, M_2, M_3\}$ and M_2 is randomly selected to O_{31}. Additionally, L in Figure 3. is the total number of operations, resulting in individuals with a chromosome coding length of $2 \times L$.

In this paper, a multi-layer decoding matrix is designed for the special AGV allocation strategy in GFJSP-MT to determine the S_{ij} and C_{ij} on machine k and calculate the individual fitness values, the steps are as follows:

Step 1: For each individual in the population, the coded values are obtained from left to right, and a series of indicators such as the t_{ijk} and TD_{ijk} are determined.

Step 2: Based on the AGV allocation strategy in Figure 1, assign AGVs to each operation, forming a 3-layer decoding matrix consisting of OS, MS, and AS. Taking two AGVs as an example, combined with Figure 3, there can be a 3-layer decoding matrix as shown in Figure 4.

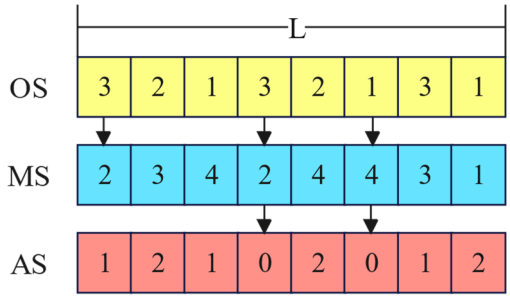

Figure 4. 3-layer decoding matrix.

Where AS is the AGV code value assigned to each operation, and the number indicates which AGV is responsible for transporting O_{ij}; for example, O_{31} is transported by the 1st AGV. AS can be seen, there is no need to assign AGVs when adjacent machining tasks on the machine k are the same job; for example, M_2 sequentially processes two operations of job_3, thus no AGV needs to be assigned to O_{32}, denoted by 0. In addition, when adjacent operations of the same job are processed on the same machine, there is no need to assign AGVs, such as O_{12}.

Step 3: Based on a 3-layer decoding matrix, metrics such as t_{ijk}, S_{ij}, C_{ij}, setup time, transport time and material consumption are embedded to calculate the individual fitness values by a multi-layer decoding matrix.

3.2. Selection

In this paper, the frequently used tournament selection operation in the NSGA-II algorithm is adopted. This operation is performed by setting up groups of population size (*NP*), randomly selecting two different individuals to form a group, and then comparing them to select the better solution. Limited by space, this paper will not elaborate more specifically.

3.3. Crossover

Based on the individual as a hybrid encoding form of operations and machines, this paper introduces the precedence operation crossover (POX) operator proposed by Zhang et al. [27]. As the POX operator only targets the operation level, this paper simultaneously adjusts the machines to achieve mixed operations and crossover on the basis of operations crossover with the following steps:

Step 1: Randomly select two different individuals of the parent generation, designated as $F1$ and $F2$.

Step 2: Randomly divide the set J into sub-sets, designated as $J1$ and $J2$, where $J1 \cup J2 = J$ and $J1 \cap J2 = \varnothing$.

Step 3: $F1$ contains the jobs of $J1$, whose operations and machines are replicated in the offspring $C1$ according to their position, and $F2$ contains the jobs of $J2$, whose operations and machines are replicated in the offspring $C2$ according to their position.

Step 4: $F1$ contains the jobs of $J2$, whose operations and machines are replicated sequentially in the offspring $C2$, and $F2$ contains the jobs of $J1$, whose operations and machines are replicated sequentially in the offspring $C1$.

As shown in Figure 5.

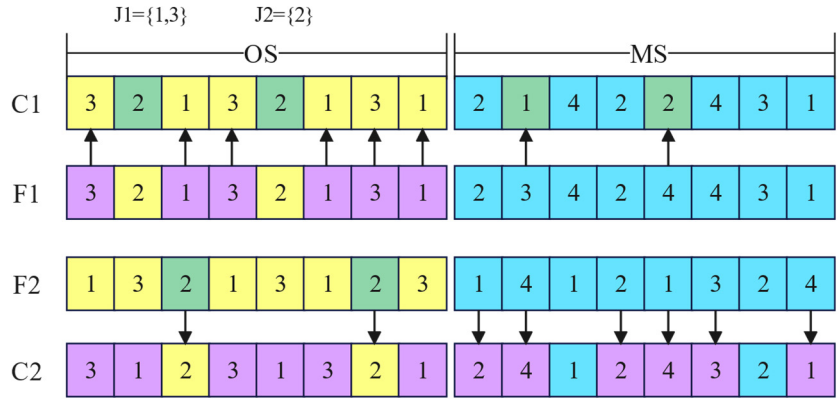

Figure 5. Mixed POX crossover of operations and machines.

3.4. Mutation

Mutation operation can expand the population search to a degree that allows the population to break out of the partial optimum; however, different mutation operators bring different degrees of change to individuals. Therefore, the mixed mutation operation will be used in this paper, i.e., one of the three mutation operators with different degrees of mutation will be chosen randomly, as shown in Figure 6, which are multiple spots interchange mutation, segment interchange mutation and reverse order mutation.

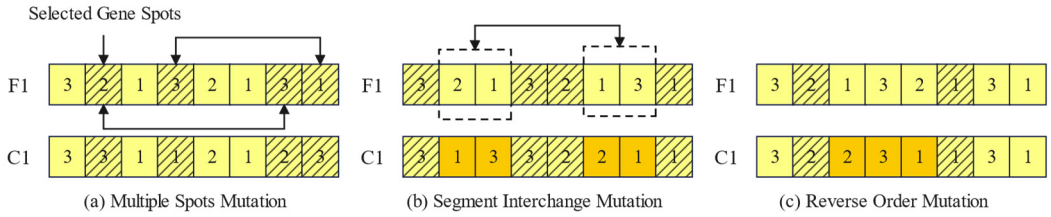

Figure 6. Mixed multiple mutation operators.

Figure 6a illustrates a random selection of four distinct gene points from the parental generation F1's OS encoding. The operation codes corresponding to gene points 1 and 3 are swapped, as are the operation codes of gene points 2 and 4. In Figure 6b, another random selection of four distinct gene points from the parental generation F1's OS encoding is presented. Here, the operation between gene point 1 and gene point 2 is interchanged with the operation between gene point 3 and gene point 4. Figure 6c showcases yet another random selection of two distinct gene points from the parental generation F1's OS encoding. Subsequently, the operation segment between these selected gene points is reversed.

These diverse mutation operations give rise to a new offspring generation, C1, with an updated operation encoding section. Lastly, it is imperative to thoroughly inspect and rectify the MS and AS encoding of the offspring generation C1 to ensure its feasibility as an independent entity.

3.5. Adaptive Operator

During the early stages of the algorithm, there is a requirement to expand the search to obtain as many high-quality individuals as possible, while in the later stages, there is a requirement to ensure that the individuals are stable towards optimal, meanwhile being able to break out of the local optimum. Therefore, this paper introduces an adaptive operator to control the crossover and mutation probabilities by the number of *gen* [28], as shown in Equations (22) and (23).

$$P_c = \min\left(P_{c\_scope}\right) + \frac{\left(\max\left(P_{c\_scope}\right) - \min\left(P_{c\_scope}\right)\right) \times \left(1 + \cos\left(\pi \times \frac{gen}{Maxgen}\right)\right)}{2} \tag{22}$$

$$P_m = \min\left(P_{m\_scope}\right) + \frac{\left(\max\left(P_{m\_scope}\right) - \min\left(P_{m\_scope}\right)\right) \times \left(1 + \sin\left(\pi \times \frac{gen}{Maxgen} - \frac{\pi}{2}\right)\right)}{2} \tag{23}$$

3.6. Heuristic Strategy

In traditional NSGA-II, after the parent and offspring are merged to obtain the population $P2$ ($2 \times NP$), there is a tendency to select NP individuals directly to form the new generation of parent population based on rank values and crowding distance. However, as the elite selection strategy of traditional NSGA-II tends to result in duplicate individuals with a crowding distance of 0 within the population, which not only predisposes the population towards a local optimum, but also reduces the diversity and quality of the Pareto solution.

Therefore, in this paper, a heuristic strategy is designed to update the population $P2$ before selecting individuals from the population $P2$ to ensure the non-duplication of individuals, as shown in Figure 7 and the steps are as follows:

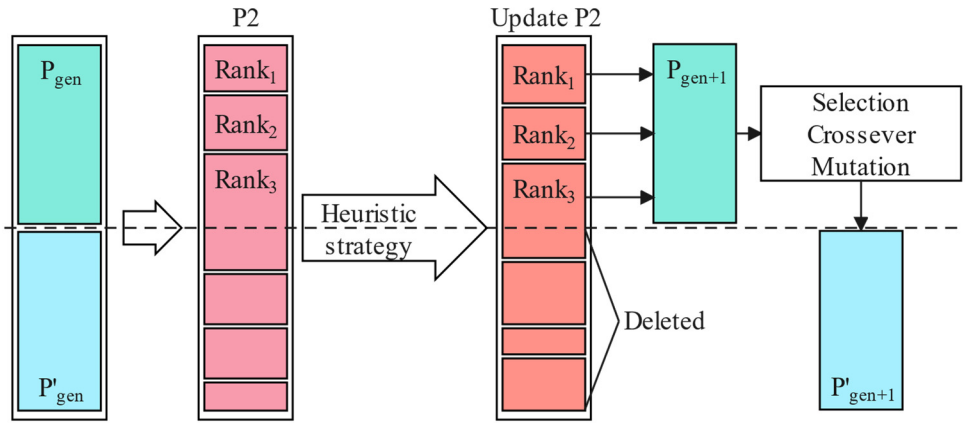

Figure 7. Merging and trimming of the populations.

Step 1: Determine whether there are individuals with a crowding distance of 0 in population $P2$, if there are, go to **Step 2**, if not, end.

Step 2: Obtain the elite individuals for $Rank_1$.

Step 3: Determine whether there is only one elite solution. If this condition is met, new individuals are obtained by crossover and mutation between elite and non-elite individuals. Otherwise, the new individuals are obtained by crossover and mutation between elite individuals.

Step 4: Duplicate individuals are replaced by optimal new individuals.

Step 5: After all duplicate individuals have been replaced, return to **Step 1**.

Step 6: After **Step 5** is completed, the population $P2$ has been updated. At this point it is required to select NP individuals from $P2$ to form a new population $P_{\text{gen}+1}$. The number of individuals allowed to be retained under each rank is constrained by Equations (24) and (25).

$$N_r = \begin{cases} |F_1|, r = 1 \;\&\; |F_1| \le (\text{Pareto Archiving Coefficient} \times NP) \\ \text{Pareto Archiving Coefficient} \times NP, r = 1 \;\&\; |F_1| > (\text{Pareto Archiving Coefficient} \times NP) \\ NP \times 0.8^{(r-1)} \times \frac{(1-0.8)}{1-0.8^R} + V_{r-1}, r \ge 2 \;\&\; |F_r| \ge NP \times 0.8^{(r-1)} \times \frac{(1-0.8)}{1-0.8^R} + V_{r-1} \\ |F_r|, r \ge 2 \;\&\; |F_r| < NP \times 0.8^{(r-1)} \times \frac{(1-0.8)}{1-0.8^R} + V_{r-1} \end{cases} \tag{24}$$

$$V_r = \begin{cases} 0, r = 1 \\ NP \times 0.8^{(r-1)} \times \frac{(1-0.8)}{1-0.8^R} + V_{r-1} - |F_r|, r \ge 2 \;\&\; |F_r| < NP \times 0.8^{(r-1)} \times \frac{(1-0.8)}{1-0.8^R} + V_{r-1} \end{cases} \tag{25}$$

where N_r indicates the number of solutions allowed to be retained for $Rank_r$, $|F_r|$ indicates the number of actual available solutions under each $Rank_r$, Pareto Archiving Coefficients is the archival retaining coefficient for the elite solutions of the $Rank_1$, R is the number of total ranks, and V_r denotes the number of solutions allowed to be retained for the overflow of $Rank_r$.

Step 7: Each sequence selects N_r solutions with maximum crowding distance by tournament.

Step 8: If the number of retained individuals is more than NP, then remove the individuals with the highest rank value and the smallest crowding distance by tournament selection again until the number of retained individuals is NP.

3.7. Non-Dominated Sorting and Crowding Distance

Non-dominated sorting has been central in NSGA-II, and as all the objective functions in this paper are minimized, the dominated relationship between two individuals can be determined according to Equation (26).

$$\exists\gamma(f_\gamma(q) < f_\gamma(p)) \& \forall\gamma(f_\gamma(q) \le f_\gamma(p)) \tag{26}$$

where p and q are two different and non-sorted individuals, respectively, and γ is the objective function. When Equation (26) is established, i.e., there exists an objective function γ of individual q that is optimal for individual p and none of the objective functions of individual q is inferior to individual p, then individual q dominates p. Conversely, p is not dominated by q and comparisons have to be made until no other individual in the population can dominate p, at which point p can be given a dominance rank.

Individual crowding distance (CD_p) is determined by individual rankings and objective functions. Namely, all individuals under each rank value and their corresponding objective functions are obtained in turn, and then for each objective function γ, a descending sort is performed, and the index of the individuals is retained. When the value of the objective function γ of individual p is minimum or maximum, its crowding distance is set to *Inf*, otherwise, each objective function γ of p is considered comprehensively and CD_p is calculated based on the neighboring individuals under each objective function of p, as shown in Equation (27).

$$CD_p = \begin{cases} Inf \\ \text{when } f_\gamma(p) = \min(f_\gamma) \text{ or } f_\gamma(p) = \max(f_\gamma) \\ \\ \sum_{\gamma}^{3} \frac{f_\gamma(p+1) - f_\gamma(p-1)}{\max(f_\gamma) - \min(f_\gamma)} \end{cases} \quad (27)$$

4. Case Study

4.1. Experimental Design

In this paper, all code was programmed using MATLAB R2013b and uploaded to Elastic Compute Service (ECS) with a 2-Core 2G Brust Performance Instance Family T6 with Windows Server 2012 R2 to run the code.

4.1.1. Data Source

The GFJSP-MT model constructed in this paper comprehensively considers machine processing power, jobs setup time, processing material consumption and AGV transport, etc. However, following a literature search, it seemed that there was a lack of relevant case sets in the academia. Therefore, the MK benchmark case proposed by Brandimarte [29] was used in this paper and combined with previous research to extend the data from actual production situations.

To begin with, the MK03 case with 15 jobs and 8 machines was selected for this paper, and the machine machining power and idle power suggested by Pirozfard et al. [15] were used for the machine power. Furthermore, as this paper considered the transport of multi-transport equipment, the machine layout was incorporated into the case set. Zhang et al. [30] investigated the layout of facilities for an energy efficient manufacturing workshop and this paper expanded on their research for a workshop layout containing 8 facilities. Eventually, Liu et al. [17] constructed a case set that incorporated job setup time and material consumption, and this paper used this template to expand the relevant production data based on the MK03 case.

4.1.2. Parameters Setting

Careful tuning of the parameter selection is of paramount importance when conducting experiments, as it directly influences the ability of the algorithm to achieve maximum efficiency. The Taguchi experiment, serving as a robust experimental design method, enables the assessment of perturbations caused by influential factors on the quality of the experimental results. By strategically combining multiple factors, Taguchi's method minimized the number of experiments required while effectively capturing the perturbations resulting from the interactions between these factors. Consequently, this approach expedited the determination of the optimal parameter combination, thus, significantly enhancing the experimental process.

The GFJSP-MT model constructed in this paper includes numerous parameters. To ensure that the proposed INSGA-II algorithm achieved maximum performance while simultaneously achieving a balanced number of AGVs in the model, it become imperative to determine the parameter selection for population size *NP*, maximum number of generations *Maxgen*, number of AGVs u, and Pareto Archiving Coefficient within this research. However, it is worth noting that the consideration of the crossover and mutation probabilities was excluded, as they were adjusted through adaptive operators. Therefore, an L25 (5^4) orthogonal experimental table was used, as shown in Table 2.

Table 2. Factor levels for parameter groups.

	Levels				
	1	**2**	**3**	**4**	**5**
population size *NP*	50	100	150	200	250
maximum number of generations *Maxgen*	100	200	300	400	500
Number of AGVs *u*	1	2	3	4	5
Pareto Archiving Coefficient	0.1	0.15	0.2	0.25	0.3

In this paper, the Inverse Generation Distance (IGD) [31] was used as a comprehensive performance evaluation metric for the Taguchi experiments, as shown in Equation (28).

$$IGD(PF, PF^*) = \frac{\sum_{S_1 \in PF^*} \min_{S_2 \in PF} (d(S_1, S_2))}{|PF^*|} \tag{28}$$

where PF^* are the true Pareto front solutions, PF is the Pareto front solutions obtained by the algorithm, $|PF^*|$ is the number of true Pareto front solutions, and d is the distance between solutions $S1$ and $S2$.

This metric evaluates the convergence and distribution performance of the algorithm by measuring the minimum distance between the PF and the PF^*. A smaller IGD value indicates a higher level of comprehensive performance, indicating superior convergence and better distribution of solutions.

Based on Table 2, 25 parameter groups were formed, and the average inverse generation distance (IGD) was used as the evaluation index, and the results are shown in Table 3.

Table 3. Orthogonal experimental results.

Parameter Groups	***NP***	***Maxgen***	***u***	**Pareto Archiving Coefficient**	**IGD**
1	50	100	1	0.1	19,339.95
2	50	200	2	0.15	12,219.93
3	50	300	3	0.2	9735.67
4	50	400	4	0.25	7883.77
5	50	500	5	0.3	7221.51
6	100	100	2	0.2	10,575.83
7	100	200	3	0.25	7625.91
8	100	300	4	0.3	6068.51
9	100	400	5	0.1	7469.12
10	100	500	1	0.15	10,117.87
11	150	100	3	0.3	9097.94
12	150	200	4	0.1	7129.66
13	150	300	5	0.15	5415.74
14	150	400	1	0.2	7661.35
15	150	500	2	0.25	3757.51
16	200	100	4	0.15	6948.34
17	200	200	5	0.2	5122.31
18	200	300	1	0.25	6943.47

Table 3. *Cont.*

Parameter Groups	*NP*	*Maxgen*	*u*	Pareto Archiving Coefficient	IGD
19	200	400	2	0.3	3487.48
20	200	500	3	0.1	4827.43
21	250	100	5	0.25	5686.09
22	250	200	1	0.3	6883.25
23	250	300	2	0.1	4546.85
24	250	400	3	0.15	3229.58
25	250	500	4	0.2	2365.62

Based on Table 3, the main effect analysis was further performed with IGD as the response and the results are shown in Figure 8. As can be concluded from Figure 8, the optimal parameter selection of this paper regarding the proposed algorithm population size *NP*, number of iterations *Maxgen*, number of AGVs *u*, and Pareto Archiving Coefficient were 250, 500, 4, and 0.25, respectively.

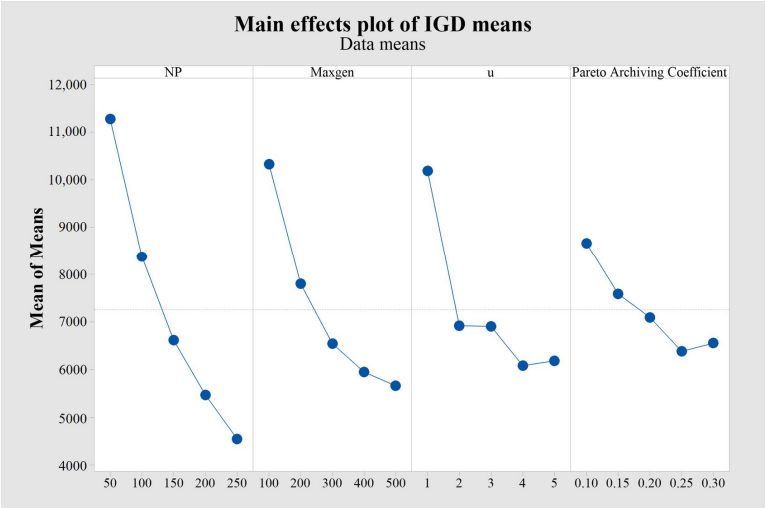

Figure 8. Main effects plot of mean IGD response.

Other parameters settings such as AGV performance are detailed in Table 4. This paper cited the carbon emissions factors value proposed by the literature [17].

Table 4. Parameters setting.

Parameters			
population size *NP*	250	Job initial-weight ϑ	30 kg
maximum number of generations *Maxgen*	500	Power coefficient η	0.95
crossover probability scope P_{c_scope}	[0.4, 0.9]	Electricity carbon emission factor EF_{α_1}	0.6981 $kgCO_2/kw{\cdot}h$
mutation probability scope P_{m_scope}	[0.01, 0.3]	Swarf carbon emission factor EF_{α_2}	3.22 $kgCO_2/kg$
number of AGVs *u*	4	Lubricant carbon emission factor EF_{α_3}	0.469 $kgCO_2/L$
AGV no-load power *q*	285 w	Coolant carbon emission factor EF_{α_4}	5.143 $kgCO_2/L$
AGV speed *V*	1 m/s	Pareto Archiving Coefficient	0.25
AGV self-weight δ	150 kg		

Additionally, along with the AGV load, the actually load power of the AGV changed; thus, this paper determined the load power p_u of the AGV according to Equation (29).

$$p_u = \frac{q \times (\delta + \vartheta_{i-current})}{\eta \times \delta} \tag{29}$$

where δ is the AGV self-weight, $\vartheta_{i-current}$ is the current weight of job_i after machining, and η is the power coefficient.

4.1.3. Aim of the Experiment

The aim of the experiment was to provide decision makers with optimal decision solutions for different objectives.

Firstly, longitudinal comparisons were made to evaluate the impact of the number of AGVs on the production system and to verify the effectiveness of the AGV allocation strategy.

Secondly, horizontal comparisons were made to validate the effectiveness and superiority of the improved NSGA-II in this paper.

4.2. Explanation of Experimental Results

4.2.1. Effectiveness of AGV Allocation Strategy

To further analyze the effects of the AGV quantity on the scheduling results and to verify the effectiveness of the AGV allocation strategy formulated in this paper. In this paper, while it maintained the consistent of the other parameters with Table 4, the optimal fitness curves of each sub-objective were formed by varying the value of the parameter u within the range of 1~5; the results are shown in Figure 9.

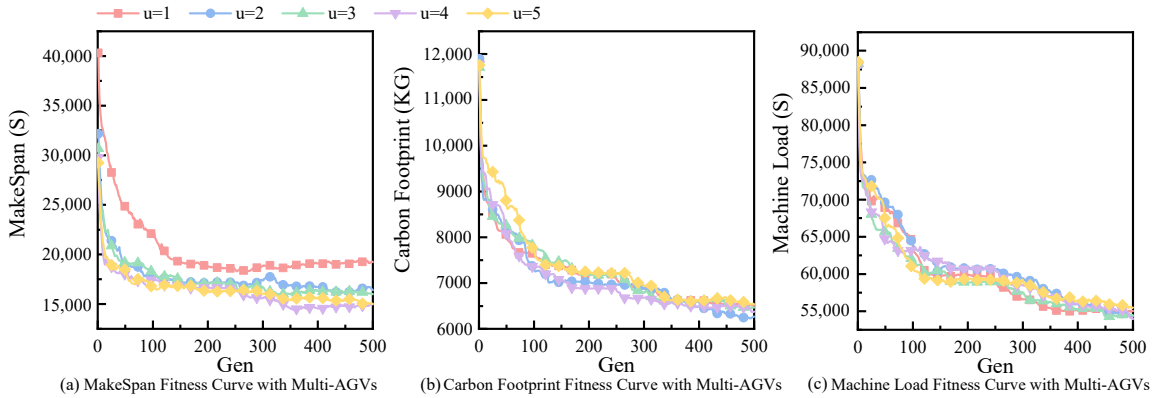

Figure 9. Generational average fitness values with multi-AGVs.

According to Figure 9a, the number of AGVs had a greater effect on the makespan, and verifies the effectiveness of the AGV allocation strategy. When merely one AGV was in transportation, the makespan was obviously at a disadvantage. In addition, the average makespan decreased as u increased, but this did not mean that the more AGVs there were the more advantageous the makespan was; for example $u = 5$ was at a disadvantage compared with $u = 4$, while $u = 3$ was not obviously better than $u = 2$.

As can be seen from Figure 9b,c, the number of AGVs seemed to have no direct effect on the total carbon footprint and total machine load. In order to further investigate the reason, the carbon emissions of each production segment were reported under a certain scheduling scheme, as shown in Figure 10.

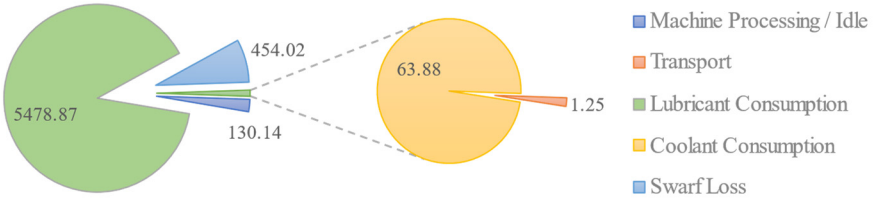

Figure 10. Carbon emissions by production segment.

It can be seen in Figure 10 that the reason the number of AGVs had no direct effect on the total carbon footprint could be due to the fact that the carbon emission from transport was only a minimal proportion, while the total machine load could be related to the selection of job processing machines.

Hence, Figure 9 shows that when $u = 4$, both in terms of makespan, carbon footprint and machine load reflect certain strengths, and coupled with the economic cost constraint, four AGVs were correctly chosen to participate in the transport, which also precisely echoes the results of the orthogonal experiment.

4.2.2. Convergence Comparison

As this paper investigates a relatively new case of GFJSP-MT, to the best of our knowledge, there have been relatively few relevant studies, so this paper would be comparative analysis between the proposed algorithm and the traditional NSGA-II and SPEA-II. The parameter settings of NSGA-II and SPEA-II were consistent with Table 4, except for the crossover and mutation probabilities, which were set to 0.85 and 0.1, respectively. The optimum population average fitness values for traditional NSGA-II and SPEA-II over generations were obtained after several experiments, and were compared with the improved NSGA-II (INSGA-II) with embedded heuristic strategy proposed in this paper; the results are shown in Figure 11.

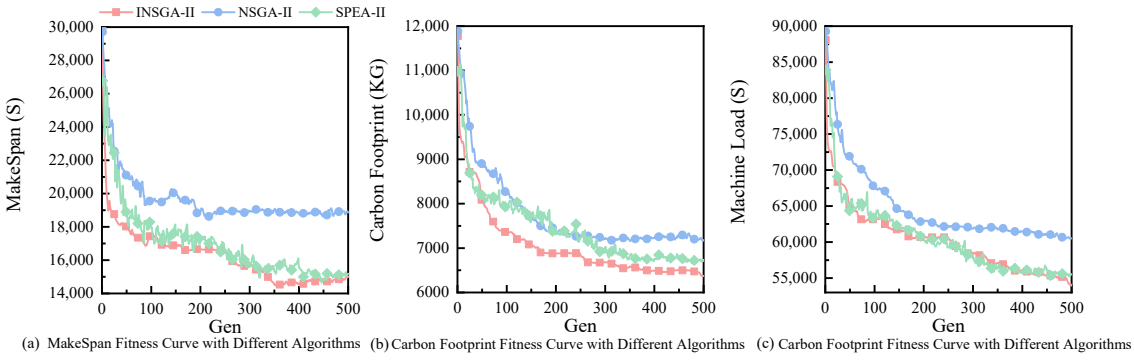

Figure 11. Comparison of average fitness values with different algorithms.

From Figure 11, it can be seen that INSGA-II was significantly superior to the traditional NSGA-II in the average fitness curves of the three sub-objectives. Additionally, INSGA-II exhibited a slight advantage over SPEA-II in terms of the completion time and carbon footprint objectives, while demonstrating comparable performance to SPEA-II in terms of machine load.

4.2.3. Pareto Comparison

Figure 12 further compares the quality and diversity of the Pareto.

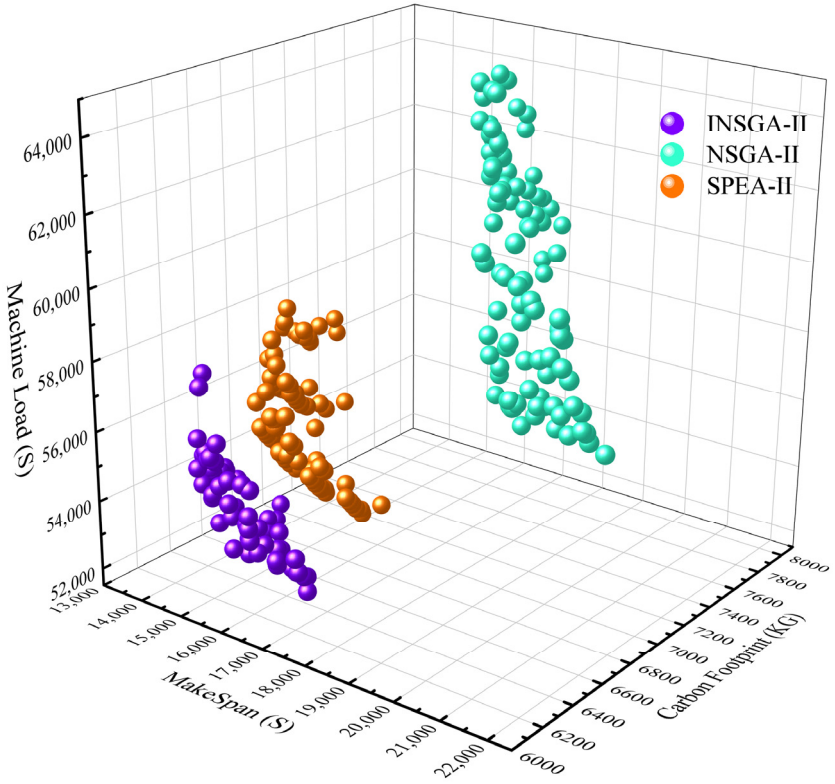

Figure 12. Pareto Quality and Diversity Comparison.

From, it can be observed that the Pareto front solutions generated by INSGA-II exhibited a slightly lower lever of diversity compared with those obtained by NSAG-II and SPEA-II. However, INSGA-II demonstrated a significant advantage in terms of solution quality. Firstly, the Quality Metric (QM) [32] was introduced, the Pareto front solutions of the three algorithms were combined and then non-dominated sorted again, and it was found that the Pareto frontier solutions of INSGA-II dominated NSGA-II and SPEA-II with 100% QM. Then, the IGD values of the PF and PF^* for INSGA-II, NSGA-II, and SPEA-II were calculated and the results were 1858.17, 7338.93, and 3508.55, respectively. In summary, the solutions obtained by INSGA-II manifested higher levels of performance and effectiveness.

4.2.4. Scheduling Scheme Discussion

However, as this paper considered a multi-objective GFJSP-MT model, the difference in sub-objectives would lead to deviations in the focus of the scheduling scheme. Therefore, in this paper, scheduling schemes with different sub-objectives were explored, aimed at providing a basis for the selection of workshop scheduling production. Firstly, the optimal scheduling scheme and fitness values for each sub-objective under $u = 4$ were given in this paper respectively, as shown in Figures 13–15. Then, the machine utilization corresponding to the scheduling scheme under each sub-objective was given, as shown in Figure 16.

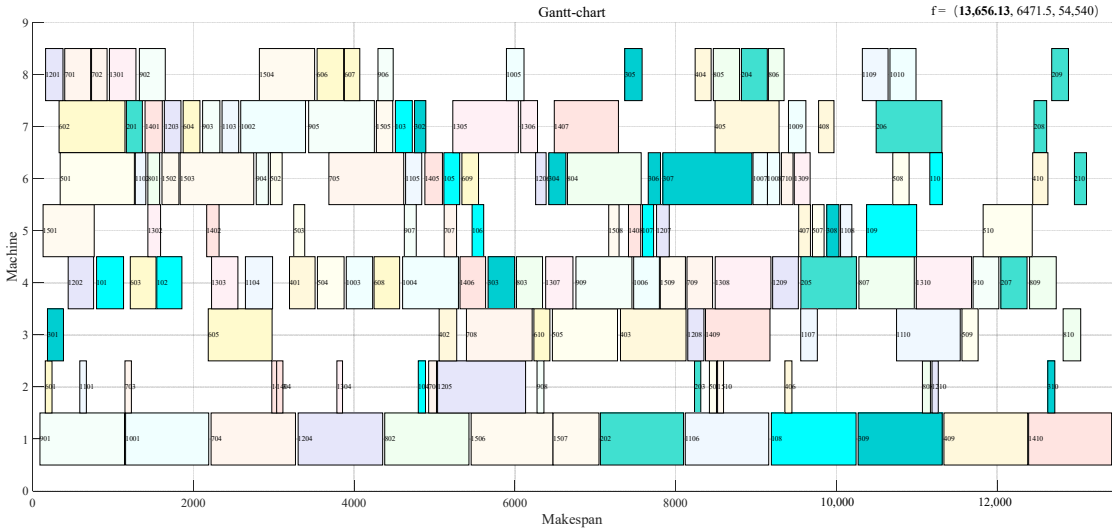

Figure 13. Gantt chart with the optimal makespan scenario.

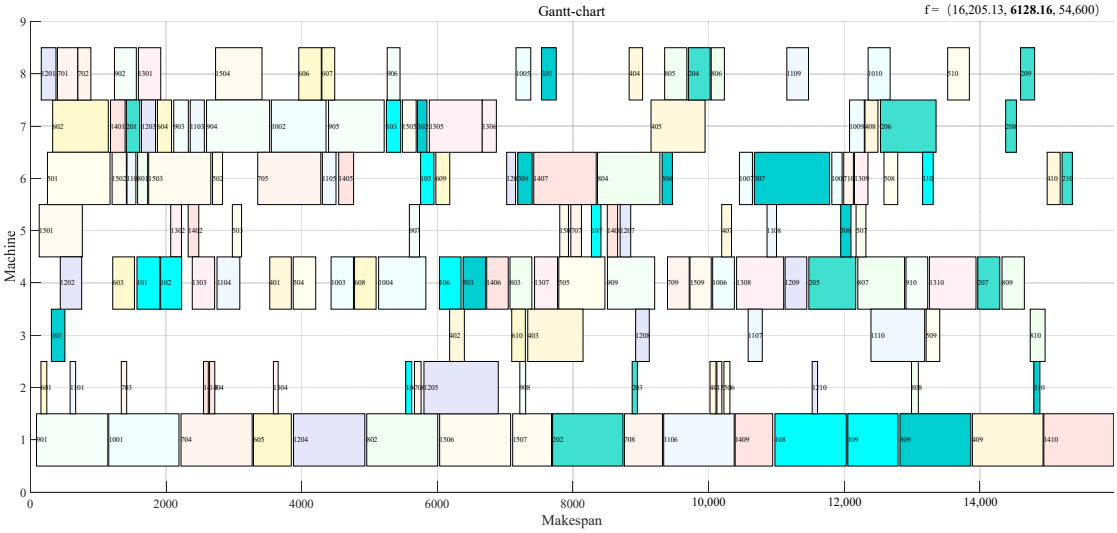

Figure 14. Gantt chart with the optimal carbon footprint scenario.

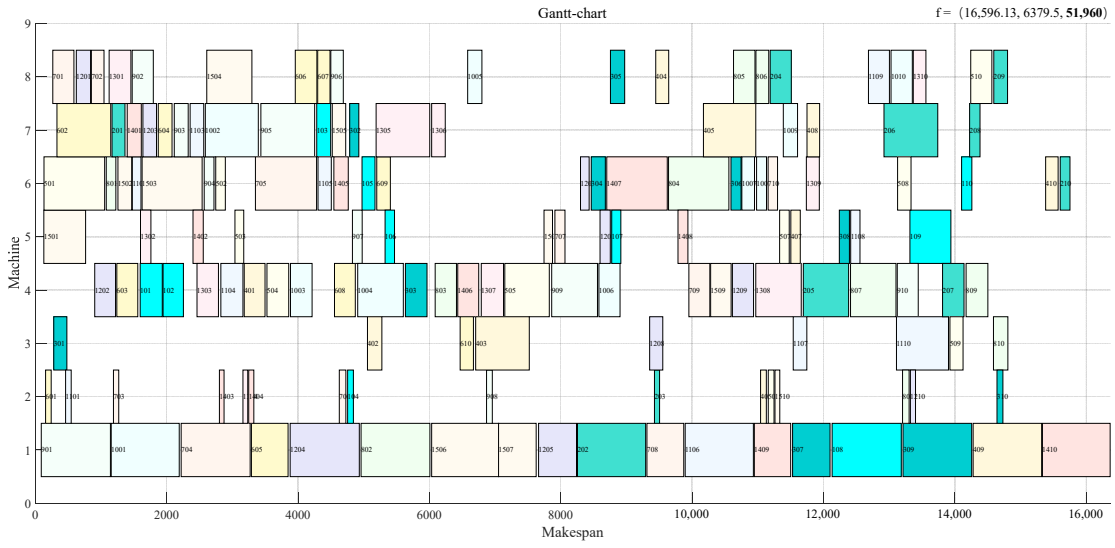

Figure 15. Gantt chart with the optimal machine load scenario.

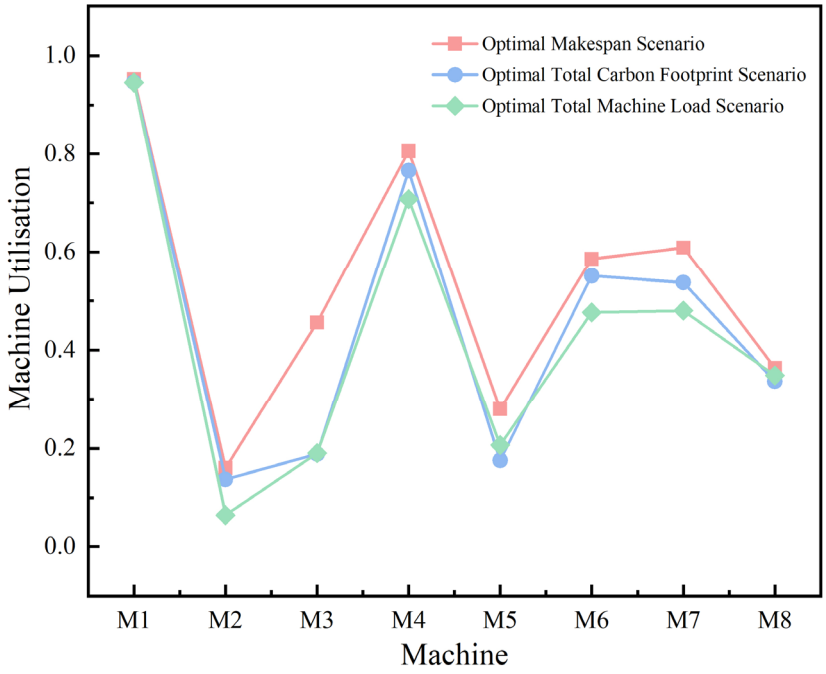

Figure 16. Machine utilization corresponding to different optimal sub-objectives.

As can be seen from Figures 13–15, the optimal scheme for the different sub-objectives correspond to fitness values of (13,656.13, 6747.5, 54,540), (16,205.13, 6128.16, 54,600), and (16,596.13, 6379.5, 51,960), respectively. It can be seen that the scheduling scheme based on optimal makespan had a significant advantage in terms of makespan, but the other two objectives were at a disadvantage, while the scheduling scheme based on the optimal total machine load only had a certain advantage in terms of machine load. In contrast, the optimal carbon footprint scheduling scheme could be balanced with the other two schemes and had a certain advantage over either one.

Similarly, Figure 16 shows that the optimal makespan scenario had an advantage in terms of utilization per machine compared with the two scenarios, but this may also be responsible for the higher carbon emissions. However, the machine utilization for the optimal carbon footprint scenario was balanced between the two scenarios. This further verifies that the optimal carbon footprint scenario could be chosen more frequently.

5. Conclusions

The implementation of sustainable and cost-effective automated production has been a significant focus of research in the field of manufacturing intelligence. Numerous factors, including job transportation strategies and the optimal number of transport equipment, have posed limitations on this endeavor. Hence, the study described in this paper holds great value and significance. Building on this basis, the paper introduces an allocation strategy for finite Automated Guided Vehicles (AGVs) by simulating various mixed processing states of jobs using the Flexible Job Shop (FJS) benchmark. After multi-dimensional analysis, the optimal number of AGVs in the case was determined and the effectiveness of the strategy was verified. Furthermore, a detailed mathematical formula for each objective was constructed with this strategy, such as the carbon footprint awareness estimation model for different bodies under the whole life cycle and job makespan model under multiple scenarios, etc. To form the GFJSP-MT, which has integrated multiple factors such as finite AGVs transport, machine layout, job setup time and job processing material consumption, and has given the relevant case data set.

Regarding the algorithm, this paper proposed an NSGA-II embedded in a heuristic strategy of replacing duplicate individuals using cross-mutation between elite solutions to address the shortcomings of the traditional NSGA-II, and the effectiveness and ad-

vantages of the proposed algorithm are demonstrated through comparative analysis of the convergence curves of fitness values and Pareto quality and diversity. At the same time, the optimal scheduling scheme for each sub-objective was discussed and it was found that the scheduling scheme based on the optimal carbon footprint could be adopted more frequently.

As this paper studied the static GFJSP-MT, which did not consider the effect of AGVs route planning on the AGVs allocation strategy and scheduling result, it also lacked dynamic factors such as machine breakdowns and new job insertions. Therefore, there may be a certain degree of deviation from the actual production.

The next steps will be in-depth research as follows:

(1) To further integrate the impact of time and route factors on AGVs allocation, and develop an AGVs allocation strategy that is more in line with actual production.
(2) Based on static scheduling, further dynamic green shop scheduling with limited AGVs transport will be explored, taking into account dynamic factors.

Author Contributions: Data curation, X.Z. and N.S.; Methodology, X.Z., F.W. and W.Z.; Founding acquisition, F.W.; Visualization, X.Z. and N.S.; Validation, F.W. and W.Z.; Writing—original draft, X.Z.; Writing—review and editing, F.W., N.S. and W.Z.; Supervision, F.W. All authors have read and agreed to the published version of the manuscript.

Funding: This research is supported by the National Natural Science Foundation of China (No. 72274001, No. 71872002), the Humanities and Social Sciences Youth Fund of Ministry of Education (No. 19YJCZH091), and the Major Project of Humanities and Social Sciences of the Education Department of Anhui Province (No. SK2020ZD16).

Data Availability Statement: The case data can be found on the website at https://pan.baidu.com/s/1s0krhid69VgYfhHeTFRKkA?pwd=xwya (accessed on 30 June 2023).

Conflicts of Interest: The authors declare no conflict of interest.

References

1. Wang, L.; Pan, Z.; Wang, J. A Review of Reinforcement Learning Based Intelligent Optimization for Manufacturing Scheduling. *Complex Syst. Model. Simul.* **2021**, *1*, 257–270. [CrossRef]
2. Destouet, C.; Tlahig, H.; Bettayeb, B.; Bélahcène, M. Flexible job shop scheduling problem under Industry 5.0: A survey on human reintegration, environmental consideration and resilience improvement. *J. Manuf. Syst.* **2023**, *67*, 155–173. [CrossRef]
3. Duan, J.G.; Wang, J.H. Energy-efficient scheduling for a flexible job shop with machine breakdowns considering machine idle time arrangement and machine speed level selection. *Comput. Ind. Eng.* **2021**, *161*, 107677. [CrossRef]
4. Caldeira, R.H.; Gnanavelbabu, A.; Vaidyanathan, T. An effective backtracking search algorithm for multi-objective flexible job shop scheduling considering new job arrivals and energy consumption. *Comput. Ind. Eng.* **2020**, *149*, 106863. [CrossRef]
5. Gong, G.L.; Chiong, R.; Deng, Q.W.; Gong, X.R.; Lin, W.H.; Han, W.W.; Zhang, L.K. A two-stage memetic algorithm for energy-efficient flexible job shop scheduling by means of decreasing the total number of machine restarts. *Swarm Evol. Comput.* **2022**, *75*, 101131. [CrossRef]
6. Lei, D.M.; Li, M.; Wang, L. A Two-Phase Meta-Heuristic for Multiobjective Flexible Job Shop Scheduling Problem with Total Energy Consumption Threshold. *IEEE Trans. Cybern.* **2019**, *49*, 1097–1107. [CrossRef]
7. Wei, Z.Z.; Liao, W.Z.; Zhang, L.Y. Hybrid energy-efficient scheduling measures for flexible job-shop problem with variable machining speeds. *Expert Syst. Appl.* **2022**, *197*, 116785. [CrossRef]
8. Wu, X.L.; Sun, Y.J. Flexible job shop green scheduling problem with multi-speed machine. *Comput. Integr. Manuf. Syst.* **2018**, *24*, 862–875. (In Chinese) [CrossRef]
9. Zhang, G.H.; Wei, S.W.; Zhang, H.J.; Lu, X.X. Optimization of flexible Job-Shop scheduling considering time and energy constraints. *Appl. Res. Comput.* **2022**, *39*, 3673–3677. (In Chinese) [CrossRef]
10. Jiang, T.H.; Deng, G.L. Optimizing the Low-Carbon Flexible Job Shop Scheduling Problem Considering Energy Consumption. *IEEE Access* **2018**, *6*, 46346–46355. [CrossRef]
11. Ning, T.; Wang, Z.; Duan, X.D.; Liu, X.D. Research on flexible job shop scheduling with low-carbon technology based on quantum bacterial foraging optimization. *Int. J. Low-Carbon Technol.* **2021**, *16*, 761–769. [CrossRef]
12. Yin, L.J.; Li, X.Y.; Gao, L.; Lu, C.; Zhang, Z. A novel mathematical model and multi-objective method for the low-carbon flexible job shop scheduling problem. *Sustain. Comput. Inform. Syst.* **2017**, *13*, 15–30. [CrossRef]
13. Zhu, H.; Deng, Q.W.; Zhang, L.K.; Hu, X.; Lin, W.H. Low carbon flexible job shop scheduling problem considering worker learning using a memetic algorithm. *Optim. Eng.* **2020**, *21*, 1691–1716. [CrossRef]

14. Seng, D.W.; Li, J.W.; Fang, X.J.; Zhang, X.F.; Chen, J. Low-Carbon Flexible Job-Shop Scheduling Based on Improved Nondominated Sorting Genetic Algorithm-II. *Int. J. Simul. Model.* **2018**, *17*, 712–723. [CrossRef]
15. Piroozfard, H.; Wong, K.Y.; Wong, W.P. Minimizing total carbon footprint and total late work criterion in flexible job shop scheduling by using an improved multi-objective genetic algorithm. *Resour. Conserv. Recy.* **2018**, *128*, 267–283. [CrossRef]
16. Jiang, Y.X.; Ji, W.X.; He, X.; Su, X. Low-carbon Scheduling of Multi-objectiove Flexible Job-shop Based on Improved NSGA-II. *China Mech. Eng.* **2022**, *33*, 2564–2577. (In Chinese) [CrossRef]
17. Liu, Q.; Tian, Y.Q.; Wang, C.; Chekem, F.Q.; Sutherland, J.W. Flexible Job-Shop Scheduling for Reduced Manufacturing Carbon Footprint. *J. Manuf. Sci. Eng.* **2018**, *140*, 061006. [CrossRef]
18. Wen, X.Y.; Sun, H.Q.; Li, H.; Qiao, D.P.; Xiao, Y.Q.; Cao, Y. Research on multi-objective green job scheduling problem based on improved NSGA-II. *J. Henan Polytech. Univ.* **2020**, *39*, 120–129. (In Chinese) [CrossRef]
19. Li, M.; Lei, D.M. An imperialist competitive algorithm with feedback for energy-efficient flexible job shop scheduling with transportation and sequence-dependent setup times. *Eng. Appl. Artif. Intell.* **2021**, *103*, 104307. [CrossRef]
20. Jiang, T.H.; Zhu, H.Q.; Liu, L.; Gong, Q.T. Energy-conscious flexible job shop scheduling problem considering transportation time and deterioration effect simultaneously. *Sustain. Comput. Inform. Syst.* **2022**, *35*, 100680. [CrossRef]
21. Li, J.Q.; Du, Y.; Tian, J.; Duan, P.Y.; Pan, Q.K. An Artificial Bee Colony Algorithm for Flexible Job Shop Scheduling with Transportation Resource Constraints. *Acta Electron. Sin.* **2021**, *49*, 324–330. (In Chinese) [CrossRef]
22. Dai, M.; Tang, D.B.; Giret, A.; Salido, M.A. Multi-objective optimization for energy-efficient flexible job shop scheduling problem with transportation constraints. *Robot. Comput. Integr. Manuf.* **2019**, *59*, 143–157. [CrossRef]
23. Wang, Y.K.; Liu, Y.B.; Wu, Y.M.; Li, S.B.; Zong, W.Z. Improved NSGA-II algorithm to solve energy-saving scheduling problem of flexible job shop considering transportation constraints. *Comput. Integr. Manuf. Syst.* **2021**. Available online: https://kns.cnki.net/kcms/detail/11.5946.tp.20210912.2002.004.html (accessed on 30 June 2023). (In Chinese)
24. Li, Y.H.; Chen, X.H.; An, Y.J.; Zhao, Z.Y.; Cao, H.G.; Jiang, J.W. Integrating machine layout, transporter allocation and worker assignment into job-shop scheduling solved by an improved non-dominated sorting genetic algorithm. *Comput. Ind. Eng.* **2023**, *179*, 109169. [CrossRef]
25. Zhang, H.L.; Qin, C.Q.; Zhang, W.H.; Xu, Z.X.; Xu, G.J.; Gao, Z.H. Energy-Saving Scheduling for Flexible Job Shop Problem with AGV Transportation Considering Emergencies. *Systems* **2023**, *11*, 103. [CrossRef]
26. Deb, K.; Pratap, A.; Agarwal, S.; Meyarivan, T. A fast and elitist multiobjective genetic algorithm: NSGA-II. *IEEE Trans. Evol. Comput.* **2002**, *6*, 182–197. [CrossRef]
27. Zhang, C.Y.; Rao, Y.Q.; Liu, X.J.; Li, P.G. An improved Genetic Algorithm for the Job Shop Scheduling Problem. *China Mech. Eng.* **2004**, *23*, 83–87. [CrossRef]
28. Song, C.X.; Ruan, J.K.; Wang, C. Flexible job shop scheduling problem based on hybrid multi-objective genetic algorithm. *J. Mech. Electr. Eng.* **2021**, *38*, 169–176. (In Chinese) [CrossRef]
29. Brandimarte, P. Routing and scheduling in a flexible job shop by tabu search. *Ann. Oper. Res.* **1993**, *41*, 157–183. [CrossRef]
30. Zhang, Z.W.; Wu, L.H.; Wu, Z.Y.; Zhang, W.Q.; Jia, S.; Peng, T. Energy-Saving Oriented Manufacturing Workshop Facility Layout: A Solution Approach Using Multi-Objective Particle Swarm Optimization. *Sustainability* **2022**, *14*, 2788. [CrossRef]
31. Tian, Y.; Cheng, R.; Zhang, X.Y.; Jin, Y.C. PlatEMO: A matlab platform for evolutionary multi-objective optimization. *IEEE Comput. Intell. Mag.* **2017**, *12*, 73–87. [CrossRef]
32. Tavakkoli-Moghaddam, R.; Azarkish, M.; Sadeghnejad-Barkousaraie, A. Solving a multi-objective job shop scheduling problem with sequence-dependent setup times by a Pareto archive PSO combined with genetic operators and VNS. *Int. J. Adv. Manuf. Technol.* **2011**, *53*, 733–750. [CrossRef]